The plumbing of Old Faithful Geyser revealed by hydrothermal tremor

Jean Vandemeulebrouck, Philippe Roux, Estelle Cros

HAL Id: hal-00806927
https://hal.science/hal-00806927

Submitted on 6 Apr 2013

The plumbing of Old Faithful Geyser revealed by hydrothermal tremor

J. Vandemeulebrouck[1], P. Roux[2], E. Cros[1]†.
[1]ISTerre, Université de Savoie, CNRS, Le Bourget du Lac, France.
[2] ISTerre, Université de Grenoble 1, CNRS, Grenoble, France
†Now at Ifremer, Plouzané France.
Corresponding author: Jean Vandemeulebrouck, ISTerre, Université de Savoie, CNRS, F-73376 Le Bourget du Lac, France. jvand@univ-savoie.fr

Key points
- Sources of hydrothermal tremor are precisely localized using acoustic array processing.
- Tracking of tremor sources reveals a lateral cavity that acts as a recharge reservoir.
- Oscillating behavior can be explained by fluid compressibility in the recharge cavity.

Index terms: Hydrothermal systems, Volcano seismology, Instruments and Techniques

Abstract: Old Faithful Geyser in Yellowstone National Park (USA) has attracted numerous scientific investigations for over two centuries in order to better understand its geological structure, the physics of its eruptions, and the controls of its intermittency. Using data acquired with a seismic array in 1992, we track the sources of hydrothermal tremor produced by boiling and cavitation inside the geyser. The location of seismic sources identifies a previously unknown lateral cavity at 15 m below the surface, on the SW side of the vent, and connected to the conduit. This reservoir is activated at the beginning of each geyser eruption cycle and plays a major role in the oscillatory behavior of the water level in the conduit before each eruption.

1. Introduction

Seismic records recorded around Old Faithful Geyser (OFG) (Fig. 1a) highlighted the remarkably energetic, seismo-acoustic activity that is induced by the continuous cavitation of steam bubbles in the water column [*Kieffer*, 1984; *Kedar et al.*, 1996]. Concurrent pressure and seismic measurements in the conduit [*Kedar et al.*, 1998], demonstrated that the boiling and cavitation is focused in the upper one meter of the water column in the conduit. Time-dependent localization of this powerful acoustic source during the eruption cycle allows us to track water level and phase separation in the conduit, which in turn provides new insight into the dynamics of the geyser.

The geometry of the Old Faithful Geyser conduit was investigated to a depth of 14 m using a video camera [*Hutchinson et al.*, 1997]. It consists of a fissure-like channel that is elongated in the eastwards direction. Video recordings show the fissure width varies with depth, and the narrowest part in the conduit, ~10 cm across, is likely responsible for the choked (supersonic) flow during the eruptions [*Kieffer*, 1989]. High temperatures and adverse flow conditions below 14 m precluded the camera from passing to deeper levels.

Based on the combination of visual observations and seismic, temperature and water level data, Kieffer [1984] recognized different stages during the OFG cycle. These stages include a ~15-min-long recharge period just after an eruption characterized by a low water level and weak seismic activity. This period is followed by a *ca*. 50-min-long period of increasing seismic activity associated with the rise of the water level prior to the next eruption (Fig. 2a).

In the present study, seismic data obtained in 1992 [*Kedar et al.*, 1996; *Kedar et al.*, 1998] with a dense array around OFG (Fig. 1b) are re-processed using acoustic localization techniques [*Legaz et al.,* 2009], with the ambition to characterize the spatial and temporal patterns of the seismic sources inside the geyser conduit (Fig. 2b).

2. Data and Localization Method

In volcano seismology, source localization is generally performed on a series of similar and individual events. However, continuous tremor activity is traditionally encountered in hydrothermal areas with high event rate (e.g., up to 100 events/min of Old Faithful), which prevents discrete seismic events from being isolated. Instead, hydrothermal tremor signals can be analyzed using beamforming techniques [*Legaz et al.,* 2009; *Cros et al.*, 2011], the goal of which is to build a probability map of the dominant acoustic source for a defined time window that might contain a large number of individual events.

A fundamental requirement for beamforming techniques [*Baggeroer et al.,* 1993] is that the signal is spatially coherent across all the geophones in the array. This implies that the selected time window is long enough to accumulate the signal-to-noise ratios from bubble collapses that occur at the same location, but not too long to prevent spatial decorrelation when the dominant noise source inside the geyser conduit shifts. An estimate of the medium's seismic velocity is also required, as velocity mismatch can degrade the resolution of the source position. This often promotes the application of beamforming techniques to low-frequency signals. In contrast, higher frequencies (short wavelength) result in a better spatial resolution of beamforming techniques. The balance between the resolution at high frequencies and the robustness at low frequencies is site specific, and is determined on a case-by-case basis.

The spatial coherence of the OFG data is optimal between 10 Hz and 15 Hz, corresponding to the lower range of the frequency spectrum that is excited by bubble cavitation in geothermal areas [*Kedar et al.*, 1998; *Legaz et al.,* 2009]. Analysis of the seismic response to hammer shots [*Kedar et al.*, 1995] reveals a mean surface velocity of ~130 m/s, slightly increasing with depth. This value was used for the velocity model, in agreement with previous studies [*Kedar et al.*, 1995; *Cros et al.*, 2011]

3. New insights on the geometry and dynamics of Old Faithful Geyser

The 137 min of recorded signals from Old Faithful were centered on a long duration eruption and were processed to locate the time-dependent dominant noise-source position. The seismic tremor signals were truncated into consecutive 20-s-long time windows, which contain at most 40 overlapping bubble collapse events.

High-resolution beamforming techniques produce a ~2 m focal spot that is much smaller than the average acoustic wavelength (λ~10 m) but still not sufficient to provide insight regarding to the diameter of the water conduit (from ~10 cm to ~1 m), especially in the constricted areas [*Cros et al.*, 2011]. Note that, as expected from a surface array, the size of the focal spot increases with depth from ~2 m for tremor sources at a depth of 10 m to ~4 m for tremors at 20 m. Taking the half of the focal spot as the acoustic resolution, the source location uncertainty ranges then from ~1 m close to the surface to ~2 m for the deeper tremor sources.

The seismo-acoustic localization of the dominant tremor source during the cycle provides information from depths greater than the 14 m reached by the video observations [*Hutchinson et*

2

al., 1997], and enables the reconstruction of both the 3D structure and the dynamics of the geyser during the eruption cycle.

The distribution of the dominant tremor sources along a SW-NE vertical plane highlights two distinct structures in the geyser subsurface where water boiling is concentrated (Figs. 1b, 3). The first structure has a cylindrical geometry and corresponds to the extension of the geyser conduit down to 20 m (Fig. 1b, black dots). At a depth of 10 m, the X-Y elongation of the noise source locations is consistent with a fissure-like conduit (Fig. 3a) that was observed *in situ* [*Hutchinson et al.*, 1997]. Note that the tremor sources in the vent between 12 m and 20 m dip towards the southwest, at an angle of ~24° (Fig. 3b). This trend points toward the vent orifice when extrapolated to the surface.

Another set of seismic sources is located at a depth range of 14 m to 28 m, which are only excited during the post-eruption recharge period. In the time-domain, these signals resemble the signals in the vent but their spectrum shows a slight shift to lower frequencies, with a central frequency decreasing by 0.5 Hz. These sources reveal a previously unknown lateral cavity-shaped structure (Fig, 1b, red dots), which is located between Old Faithful Geyser and Split Cone, a weakly active geyser to the southwest (Fig. 3a). The flat roof of this structure, at ~15 m below the surface (Fig. 3b) clearly stands out as the upper horizontal boundary of the seismic tremor location, and may correspond to a lithological boundary, e.g. the base of the sinter layer.

This deep structure, composed of a sub-vertical conduit connected at depth to a lateral sub-horizontal cavity is similar to first models of geyser with a siphon-like conduit connected to a bubble trap [*Mackenzie*, 1811] and to horizontal bubble-trap structures in Kamchatka geysers inferred from video images [*Belousov et al.*, 2013]. The temporal link between the geyser vent and the "recharge cavity" is evident from depth variations of the dominant tremor sources shown in Figure 2b. The location of seismic sources in the cavity area during the 15 min following the eruption (Fig. 1b, red dots) indicates the recharge of this deep structure. After this stage, the tremor sources slowly rise towards the geyser conduit, following an exponential time-dependence (Fig. 2b), up to a depth of ~10 m. The temporal evolution of the tremor source shows recurrent periods of water level stability at this depth, which has already been observed [*Kedar et al.*, 1996] at Old Faithful. It was explained by the enlargement of the conduit at a depth of 10 m, which forces the water level in the conduit to be nearly constant even though water is still filling the conduit (Fig. 4). This steady hydraulic state is generally followed by an unstable period in which some variability can occur both in the location of the source and in the amplitude of the seismic signal. This stage finally leads to an eruption, when the strong seismic signal observed at the surface is due to water splashing at the surface near the geophones.

In the data record, there is an initial rising phase that occurs 45 min before eruption. This ends with the sudden return of the seismic sources from the geyser conduit to the recharge zone, with no eruption and splashing at the surface. This could indicate an aborted eruption that would be in agreement with the bimodal eruption cycle observed by *Kieffer* (1984).

Periods of rising dominant tremor sources in the geyser conduit can be closely matched with an exponential function (Fig. 2b). During the initial rising cycle, the characteristic time (12.5 +/- 2 minutes) is twice as long as in the following two cycles (6.3 +/- 2.3 minutes), and the critical depth of 10 m is not reached. This could explain why no eruption is observed during this cycle. The amount of water filling and its rate are governed by the hydraulic boundary conditions, and these depend on the volume of water discharged during the previous eruption. This behavior, whereby the triggering of an eruption depends on the amount and rate of water filling in the geyser (Steinberg, 1999), could be an explanation for the bimodal distribution of the eruption interval.

4. Discussion

During the stable periods with tremor sources at a depth of ~10 m, the sources have harmonic oscillations with amplitudes of about 1 m, and periods of 1 min (Fig. 4a). Similar periodic water temperature oscillations were observed [*Hutchinson et al.*, 1997] using temperature probes lowered into the conduit, and explained to result from convective instability. We suggest that this periodic instability results from free oscillations [*Berest et al.,* 1996] of a column of liquid water in the conduit above a compressible steam-rich fluid region in the recharge cavity, which has the role of a bubble trap.

Indeed, water in the upper part of the conduit (Fig. 3c) can be considered as a rigid mass that moves up and down as if above a spring, with this movement obeying the classical harmonic equation. The period of oscillation (*T*) depends on the geometry and compressibility of the spring-equivalent region, and this can be described by $T = 2\pi/\omega$, where $\omega^2 = \dfrac{S}{V\beta\rho h}$, and S is the cross-section of the conduit, h is the height of the liquid mass of density ρ, V is the volume of the cavity, and β is the compressibility of the fluid in the cavity. For slow pressure variations, the compressibility β can be written as $1/(\gamma p_2)$, where $\gamma \approx 1.3$ for steam, and p_2 is the hydrostatic pressure in the cavity.

A conduit diameter of ~0.1 m (as observed in videos at depths of 7 or 10 m), a gas-filled cavity at 15 m in depth, with volume ~62 m^3 and a 4 m characteristic size that fits with the seismic structure revealed in Fig. 3b would give the observed oscillation period of $T = 60$ s. It may be noted that pockets of air trapped in the horizontal enlargement of the upper conduit can act as additional barometric springs. The cavity volume inferred from this study is larger than the erupted volume at OFG, which was estimated from 20 m^3 [Kieffer, 1984] to 40 m^3 [Allen and Day, 1935], in agreement with the observation that several consecutive eruptions were required to clear OFG from an introduced tracer [Fournier, 1969].

As shown in Figure 4, the oscillation pattern is observed simultaneously in the depth of the seismic source, the seismic intensity and the central frequency of the seismic records. During an oscillation, water level rise (Fig. 4a) corresponds to fluid pressure increase, which causes a decrease in bubble diameter at the top of the water column. If a constant steam-injection rate during this stability period is assumed, then these smaller bubbles can induce both (1) a larger number of bubbles, to maintain a constant gas volume, and which implies a stronger seismic intensity (Fig. 4b), and (2) an increase in the central frequency of the seismic records (Fig. 4c).

In summary, these time-varying locations of seismic hydrothermal tremor source suggest that there is a compressible fluid-filled cavity at depth in the 'plumbing' system that can produce free oscillations of a water column that is excited by hydrodynamic pressure transients. This water level oscillation in the conduit is of fundamental importance for eruption triggering, as it favors water overflowing from the vent when the water level is close to the surface. Successive overflowing episodes constitute the preplay stage [*Kieffer*, 1984], which induces boiling by reducing the hydrostatic pressure in the conduit that triggers the eruption.

5. Conclusion

In conclusion, data from dense seismic arrays surrounding very energetic seismic radiators such as geysers that are processed with precise localization techniques enable detailed

mapping of structures in hydrothermal systems. This in turn allows monitoring of multiphase fluid flow in the system, which improves our knowledge of geyser dynamics. In recent models of geyser dynamics, the existence of a constriction in the vertical conduit [*Kieffer*, 1984] or of high-permeability contrast in the fractured rock medium [*Ingebritsen and Rojstaczer*, 1993] was necessary to explain the generation of the flow intermittency in geysers. In this study, the presence of a subterranean lateral cavity revealed by the location of hydrothermal tremor sources during a cycle eruption appears to play a major role in the eruptive dynamics of Old Faithful Geyser.

References

Allen, E. T., and A. L. Day (1935), Hot Springs of the Yellowstone National Park, *Carnegie Inst. Washington Publ., 466*, 525 pp.

Baggeroer, A. B., W. A. Kuperman, and P. N. Mikhalevsky (1993), An overview of matched field methods in ocean acoustics, *IEEE J. Oceanic Eng., 18,* 401-424.

Belousov, A., M. Belousova, and A. Nechayev (2013) Video observations inside conduits of erupting geysers in Kamchatka, Russia, and their geological framework: implications to the geyser mechanism. *Geology*, *doi:10.1130/G33366.1*.

Berest, P., J. Bergues, and B. Brouard (1996), Vibrations and free oscillations in salt caverns, *Solution Mining Research Institute Fall Meeting*, Cleveland, Ohio, 20-23 Oct. 1996, 311-335.

Cros, E., *et al.* (2011), Locating hydrothermal acoustic sources at Old Faithful Geyser using Matched Field Processing, *Geophys. J. Int., 187*, 385-393.

Fournier R. O. (1969), Old Faithful: A Physical Model, *Science, 163*, 304-305.

Hutchinson, R. A., J. A. Westphal, and S. W. Kieffer (1997), *In-situ* observations of Old Faithful Geyser, *Geology, 25*, 875-878.

Ingebritsen, S., and S. Rojstaczer (1993), Controls on geyser periodicity, *Science, 262*, 889-892.

Kedar, S., B. Sturtevant, and H. Kanamori (1996), The origin of harmonic tremor at Old Faithful Geyser, *Nature, 379*, 708-711.

Kedar, S., H. Kanamori, and B. Sturtevant (1998), Bubble collapse as the source of tremor at Old Faithful Geyser, *J. Geophys. Res.***,** *103*, 24283-24299.

Kieffer, S. (1984), Seismicity at Old Faithful Geyser: an isolated source of geothermal noise and possible analogue of volcanic seismicity, *J. Volcanol. Geotherm. Res., 22*, 59-95.

Kieffer, S. (1989), Geologic nozzles, *Rev. Geophys., 27,* 3-38.

Legaz A. *et al.* (2009), Self-potential and passive seismic monitoring of hydrothermal activity: a case study at Iodine Pool, Waimangu geothermal valley, New Zealand, *J. Volcanol. Geotherm.*

Res., 179, 11-18.

Mackenzie G. P. (1811), *Travels in the Island of Iceland* (T. Allan, Edinburgh).

Steinberg, A.S. (1999), An experimental study of geyser eruption periodicity, *Power engineering*, *366*, 47-50.

Figure captions

Fig. 1. Seismic array and 3D representation of the hydrothermal tremor sources at Old Faithful Geyser (OFG). (A) Shaded relief map of OFG area, with UTM coordinates (m). The red square indicates the study area. (B) Elevation model (with 1-m-interval in color) and position of the 96 vertical geophones (+), with reference to OFG vent. SC refers to Split Cone geyser. The location of the dominant seismic sources at depth discriminates between two structures: the geyser conduit and its vertical downward extension (black dots) and a lateral, cavity-shape structure (red dots).

Fig. 2. Time variation of the tremor amplitude and depth of the dominant tremor source. (A) Normalized root-mean-square amplitude averaged over the whole network. The gray rectangle with higher amplitudes corresponds to water splashing at the surface during the geyser eruption. The steady period during which water level oscillations are observed (see Fig. 4) is delimited by the two vertical dashed lines. (B) Depth-*versus*-time location of the tremor sources after beamforming, over three successive geyser cycles. The black dots correspond to tremor sources located in the geyser conduit, and the red dots to tremor sources in the recharge cavity (see Figs. 1 and 3). The dotted blue lines correspond to the exponential fit of the water level rising periods in the geyser conduit.

Fig. 3. Spatial representation of the tremor sources obtained from beamforming and the proposed structure of OFG reservoir. **(A)** X-Y projection of the tremor sources showing the sources inside the geyser conduit (black dots) and the sources in the recharge cavity (red dots). The insert corresponds to the X-Y elliptic shape of the cluster of tremor sources in the fissure-like conduit (from 12 m to 20 m; dashed line), to be compared to the X-Y elongation observed at the surface (full line). **(B)** Vertical projection of the noise sources along the OFG-SC segment and proposed model of structure, with a sub-vertical conduit connected to a lateral cavity. The flat roof of the recharge cavity is clearly highlighted by the density of red dots. The upper part of the conduit and the constriction are adapted from *Hutchinson et al.* [1997], the widening at about 10 m depth is represented as horizontal fractures. **(C)** Schematic diagram of an oscillating liquid-water column over a compressible bubble-trap cavity, equivalent to a mass-spring harmonic oscillator.

Fig. 4. Harmonic oscillations observed over a 5-min-long interval in a steady period (see Figure 2A). The blue stars correspond to data points. The black line is a band-passed filtered interpolation. (A) Depth-versus-time of the tremor sources. (B) Root-mean square amplitude recorded by the geophones around the vent. (C) Time evolution of the central frequency change of the seismic tremor.
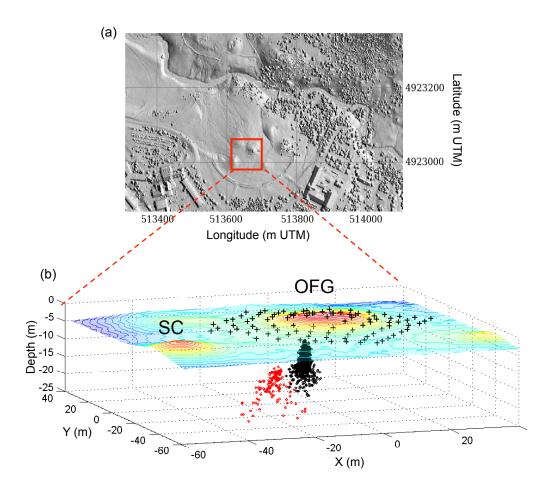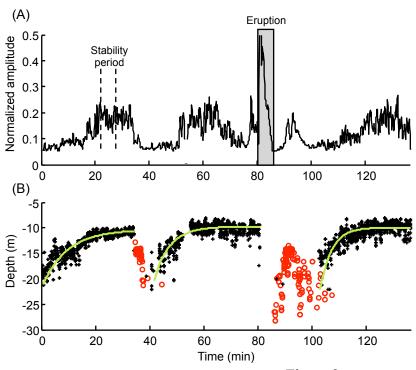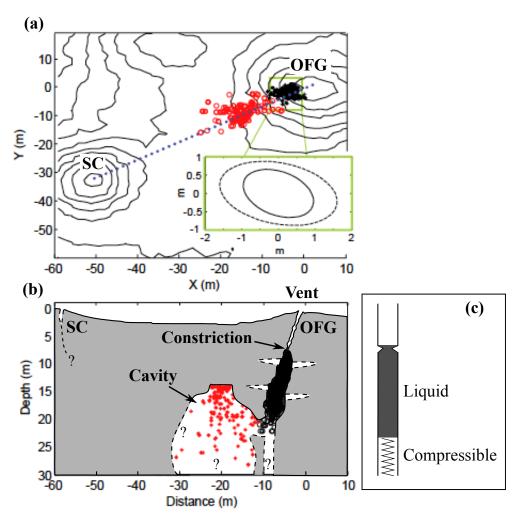
Figure 1

Figure 2

Figure 3

Figure 4